Theoretical prediction of the performance of a PEM Fuel Cell with consideration of the ageing effect on catalytic activity and conductivity of the membrane

Rao, S.S.L.
Department of Mechanical Engineering,
National Institute of Technology Calicut,
Kerala, India-673601

Shaija, A.
Department of Mechanical Engineering,
National Institute of Technology Calicut,
Kerala, India-673601

Jayaraj, S.
Department of Mechanical Engineering,
National Institute of Technology Calicut,
Kerala, India-673601

Abstract -   A mathematical model for the analysis of proton exchange membrane fuel cells is proposed. A special feature of this model is that the voltage degradation due to changes in the catalytic activity and resistivity of the membrane with ageing has been introduced in the model. The membrane used in Proton Exchange Membrane (PEM) fuel cell is Nafion. Its properties like proton conductivity, hydrophobicity and gas permeability are time dependant. Moreover, at the beginning-of-life, Gas Diffusion Layer (GDL) exhibits hydrophobic characteristics and over prolonged fuel cell operation it loses hydrophobicity and becomes more hydrophilic. This may cause voltage degradation due to changes in the catalytic activity. The effects of operating parameters and cell parameters on the performance of the fuel cell are studied. The model has been validated with experimental results at three different temperatures and the comparison shows that there is a good agreement between experimental data and the model.

Keywords- Fuel cell overpotentials; Performance Analysis; PEM Fuel Cells; Voltage degradation.

I. INTRODUCTION

In recent years, the demand for environmentally friendly and cost effective alternatives to conventional power sources has significantly grown. As a result, many countries have invested considerable resources in finding and implementing new methods of power production. One of the new technologies under consideration, which is energy efficient, low pollutant emissions, and has an unlimited supply of energy, is a fuel cell. Still a maturing technology, fuel-cell technology has already shown its advantages, such as its high-energy conversion efficiency, modular design and very low environmental pollution, over conventional power generation equipments. Fuel cells are now closer to commercialization than ever and they have the ability to fulfil all of the global power needs while meeting the efficacy and environmental expectations. Among all kinds of fuel cells, PEM fuel cells are compact, lightweight, operate at relatively low temperatures with a high output power density, and offer superior system start-up and shutdown performances. These advantages have sparked development efforts in the fields of applications for PEM fuel cells which includes, transportation, power supply, compact cogeneration stationary power supply, portable power supply and emergency and disaster backup power supply.

Fuel cell modelling helps the fuel cell developers because it can lead to fuel cell design improvements, develop cheaper, better and more efficient fuel cells. Two key issues limiting the commercialization of fuel cell technology are better performance and lower cost. The performance of a fuel cell can be illustrated by a polarization curve (i.e. voltage versus current density plot). The polarization curve is divided into three regions characterized by activation overpotential, ohmic overpotential and concentration overpotential. Activation overpotential represents voltage which is sacrificed to overcome the activation barrier associated with the electrochemical reaction, ohmic overpotential arises from the resistance of the materials for the charge transport

used in the fuel cell and concentration overpotential occurs when the chemical reaction is limited by the rate at which reactants can be supplied. The performance of a fuel cell is limited by these polarizations.

Most of the research work reported has concentrated on the design and performance modelling of the PEM fuel cells. The electrolyte used in PEM fuel cell is a solid polymer membrane and the catalyst is Platinum which is the most active catalyst for low-temperature fuel cells. The studies which are conducted mathematically predicted long term performance of the fuel cells, relied on the time independent virgin properties of the polymeric materials employed in PEM fuel cells. However, the properties of the PEM can significantly change as a function of time and temperature due to degradation or ageing which could be either of chemical or physical nature. Chemical degradation which occurs due to a harsh chemical environment may result in the loss of functional sulphonic acid groups attached to the fully fluorinated backbone and scissoring of the backbone itself. Both processes affect the proton conductivity, mechanical stability, hydrophobicity and gas permeability of the membrane. Physical degradation which occurs due to clamping pressure, operating temperature and stress also affects the mechanical properties of the membrane [1].

Several researchers have developed different models for the analysis of a single PEM fuel cell considering different parameters and approaches. Springer *et al.* [2] have used an analytical approach where only the losses incurred by the cathode reaction and the membrane are considered. The membrane model have allowed for variable hydration between the anode and cathode and thus variable ohmic resistance due to the hydration of the membrane. An empirical formula was used to relate the hydration of the membrane and the conductivity. Bernardi and Verbrugge [3] have used an analytical approach to develop a mathematical model of a PEM fuel cell from the fundamental transport properties where the losses due to the activation overpotential incurred by the anode and cathode, ohmic overpotential incurred by the membrane due to the electrodes are subtracted from the reversible cell voltage. But this model does not account for the concentration overpotential region of the polarization curve. The membrane is assumed to be fully flooded and the void regions of the catalyst layer are assumed to contain membrane phase only. Amphlett *et al.* [4, 5] have developed a mechanistic and empirical model for the Ballard Mark IV fuel cell that combines the performance losses into the parametric equations based on the operating pressure and temperature of the fuel cell. This model also does not consider the concentration overpotential region. Kim *et al.* [6] have developed an empirical equation based on the experimental data which is shown to fit the entire polarization curve of a PEM fuel cell. The models developed by the above mentioned researchers are not easily applicable to fuel cells with different characteristics and dimensions, since they have not included the length or area in their models. Mann *et al.* [7] have presented a general electrochemical model that accept input values of cell parameters such as active area and membrane thickness in addition to the operating parameters like anode and cathode feed gas pressure and compositions, cell temperature and current density. Fowler *et al.* [8] have incorporated voltage degradation term which significantly reduces the electrochemical power into the generalised electrochemical model developed by Mann *et al.* [7]. Maxoulis *et al.* [9] have presented a semi empirical model based on equations developed by Amphlett *et al.* [4,5] for automotive fuel cell operation. Al-Baghdadi [10] have developed a model for the analysis of a PEM fuel cell based on semi empirical equations developed by Amphlett *et al.* [4,5] for activation overpotential and Mann *et al.* [7] for ohmic overpotential. Youssef *et al.* [11] have developed a lumped model for PEM fuel cell and studied the effect of parameters like temperature, membrane thickness and GDL thickness on the cell performance. Mert, Dincer and Ozcelik [12] have presented a performance analysis of a PEM fuel cell engine system used for transport applications to investigate how the system performance is affected by the system operating parameters, such as operating pressure and temperature, membrane thickness, anode stoichiometry, cathode stoichiometry, humidity and reference temperature and pressure. Since proton conductivity, hydrophobicity and gas permeability of the membrane depends on the physical ageing of the MEA; introducing membrane ageing term in the present model makes it special. According to the free volume theory, "holes" or free volume must be present in the membrane between polymeric chain segments for the molecular motion to occur. As the free volume reduces with time, the mobility of species within the chain also decreases reducing the diffusion coefficients for water and proton transport [13]. Therefore, in the present model, the voltage degradation due to changes in the catalytic activity and resistivity of the membrane with ageing has also been accounted for in the analysis of PEM fuel cells by changing the different operating parameters and cell parameters.

II. METHODOLOGY

In the present work, a mathematical model has been developed for the analysis of PEM fuel cell based on the mechanistic and empirical models developed by Mann *et al.* [7], also considering the concentration overpotential, developed by Guzella [14] which uses nonlinear regression with polarization data obtained from an automotive propulsion-sized PEM fuel cell stack. Since the concentration overpotential occurs generally at higher current densities, it may be neglected for a single fuel cell, as higher current densities are not reached. However, it may not be avoided for a fuel cell stack employed for practical applications.

As reported in the literature, GDL in fuel cell losses its hydrophobicity over prolonged operation and becomes hydrophilic, which causes voltage degradation due to the changes in the catalytic activity and the properties of

the membrane are time-dependant. Thus the voltage degradation terms developed by Fowler et al. [8] to account for ageing of the MEA has also been included in this model.These terms take care of the changes in the catalytic activty of the catalyst layer and water carrying capacity of the membrane with time-in-service.

The present mathematical model developed also take into account, the effect of the major operating parameters such as anode and cathode feed gas pressure and compositions, cell temperature, current density, and the cell parameters like area, membrane thickness, water content in the membrane on the overpotentials, polarization, power density and efficiency of the fuel cell. The present model has been validated with the experimental results of Ballard MK5-E proton exchange membrane fuel cell (PEMFC) stack at three different temperatures presented by Laurencelle *et al.* [15]. The comparison shows that there is a good agreement between experimental data and the model.

III. MODEL FORMULATION

A typical PEM fuel cell, as shown in Figure 1 consists of a negatively charged electrode (anode), a positively charged electrode (cathode) and a proton conducting electrolyte membrane. Hydrogen gas under pressure is supplied to the flow field of anode where oxidation of Hydrogen takes place. Hydrogen ions (protons) produced is transported from anode to cathode through the electrolyte membrane and electrons are carried to the cathode over the external circuit or load resulting in the current flow. On the other side, Oxygen gas is supplied to the flow field of cathode where reduction of oxygen takes place and forms water after combining with protons and electrons. At the surface of two electrodes, the electrochemical reactions takes place as shown in Equations (1) and (2), and the overall reaction shows that the output from a fuel cell is water, heat and electric current as shown in Equation (3).

Anode reaction (HOR): $\quad H_2 \rightarrow 2H^+ + 2e^-$ (1)

Cathode reaction (ORR): $\quad \frac{1}{2}O_2 + 2H^+ + 2e^- \rightarrow H_2O$ (2)

Overall reaction: $\quad H_2 + \frac{1}{2}O_2 \rightarrow H_2O + \text{Electrical energy} + \text{Waste heat}$ (3)
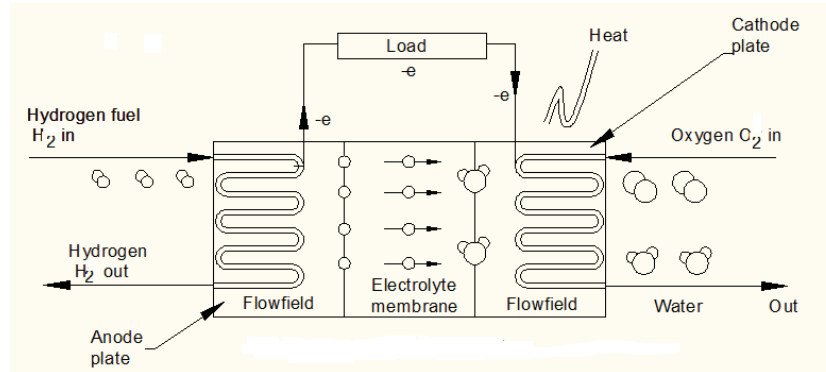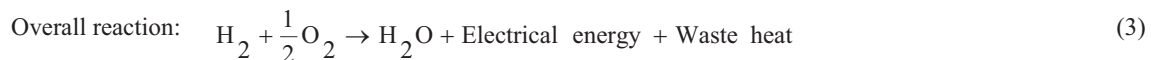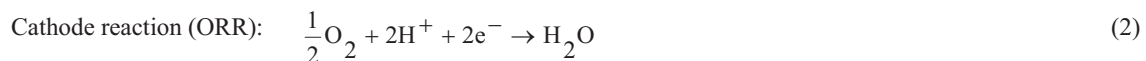

Fig.1 Schematic of a PEM fuel cell.

One of the reasons for fuel cell modelling is to determine why the actual voltage of the fuel cell is different from the thermodynamically predicted theoretical voltage. The maximum possible fuel cell potential is achieved when it is operated under thermodynamically reversible condition. The actual fuel cell potential (V) is decreased from its equilibrium thermodynamic potential (E), also called open circuit voltage, because of the irreversible losses. These losses which cause deviation from the equilibrium value are called the overpotential, denoted by η, which are primarily, activation overpotential (η_{act}), ohmic overpotential (η_{ohmic}) and concentration overpotential (η_{con}). The operating voltage of a cell can be represented as the departure from ideal voltage caused by these polarizations.

$$V = E + \eta_{act} + \eta_{ohmic} + \eta_{conc}$$ (4)

A. Open Circuit Voltage

The open circuit voltage (E) is calculated using the energy balance between the products and reactants and the Faradays Constant is given by the Nernst equation [16]:

$$E = E_0 - \frac{RT}{2F} \ln[\frac{1}{p^*_{H_2}(p^*_{O_2})^{0.5}}] \tag{5}$$

Further this equation is modified by Amphlett et al. [4] by substituting the values of E_0, R and F

$$E = 1.229 - 8.5 \times 10^{-4}(T - 298.15) + 4.3085 \times 10^{-5}T[\ln[(p^*_{H_2}) + \frac{1}{2}\ln(p^*_{O_2})]] \tag{6}$$

The partial pressure of Hydrogen and Oxygen given by Spiegel [17] is as follows:

$$p^*_{H_2} = 0.5 \times \frac{P_a}{1.0325 \times \exp(1.653 \times \frac{i}{T^{1.334}})} - P_{H_2O} \tag{7}$$

$$p^*_{O_2} = 0.5 \times \frac{P_c}{1.0325 \times \exp(4.192 \times \frac{i}{T^{1.334}})} - P_{H_2O} \tag{8}$$

Where, the saturation pressure of water vapour is calculated by Springer et al. [2] as:

$$\log P_{H_2O} = -2.1794 + 0.02953 \times t - 9.1837 \times 10^{-5} \times t^2 + 1.4454 \times 10^{-7} \times t^3 \tag{9}$$

B. *Activation Overpotential*

On the catalyst surfaces the bond in the H_2 and O_2 molecules are broken and new bonds are formed to produce water which needs energy and causes voltage drop called the activation overpotential. Activation overpotential represents voltage which is sacrificed to overcome the activation barrier associated with the electrochemical reaction, or in other words, it is the energy lost due to the slowness of electrochemical reactions at the anode and the cathode electrodes. Therefore, more current drawn from the fuel cell will be at the expense of voltage loss or activation overpotential. This dominates at the low current density region and is almost constant during when moderate current is drawn from the fuel cell as shown in Figure 2. The activation overpotential is represented by the following expression in parametric form by Amphlett et al. [4]

$$\eta_{act} = \xi_1 + \xi_2 T + \xi_3 T[\ln(C^*_{O_2})] + \xi_4 T[\ln(I)] \tag{10}$$

Where ξ_i are the semi empirical coefficients defined by the following equations [4]

$$\xi_1 = (\frac{-\Delta F_e}{\alpha_c nF}) + (\frac{-\Delta F_{ec}}{2F}) \tag{11}$$

$$\xi_2 = \frac{R}{\alpha_c nF} \ln[nFAk^0_c (C^*_{H^+})^{(1-\alpha_c)} (C^*_{H_2O})^{(\alpha_c)}] + \frac{R}{2F}[\ln(4FAk^0_a C^*_{H_2})] \tag{12}$$

$$\xi_3 = \frac{R}{\alpha_c nF}(1-\alpha_c) \tag{13}$$

$$\xi_4 = -(\frac{R}{\alpha_c nF} + \frac{R}{2F}) \tag{14}$$

The parametric expression for the activation overpotential resulting from a linear regression of three factor model given by Amphlett et al [4] is:

$$\eta_{act} = -0.9514 + 0.00312T + 7.4 \times 10^{-5}T[\ln(C^*_{O_2})] - 0.000187T[\ln(I)] \tag{15}$$

Where $C^*_{O_2}$ is the concentration of dissolved oxygen at the gas/liquid interface and can be defined by Henry's law:

$$C^*_{O_2} = \frac{p^*_{O_2}}{5.08 \times 10^6 \exp(\frac{-498}{T})} \tag{16}$$

The activation overpotential shown in Equation (15) is developed by assuming constant cell active area by assuming cross-sectional area as 232 cm^2 and hence not suitable for any other dimensions of cell active area. Amphlett et al. [4] also assumed the concentration of hydrogen at anode membrane interface as constant which

otherwise depends on partial pressure of hydrogen and temperature of fuel cell. Therefore, Mann et al. [7] proposed the following values of the coefficients for their generalised steady state electrochemical model which could take other input values of cell active area and concentration of hydrogen:

$$\xi_1 = -0.948(\pm 0.004) \tag{17}$$

$$\xi_2 = k_{cell} + 0.000197\ln(A) + 4.3 \times 10^{-5}\ln(C_{H2}^*) \tag{18}$$

$$\xi_3 = 6.8 \pm 0.2 \times 10^{-5} \tag{19}$$

$$\xi_4 = -1.97 \pm 0.05 \times 10^{-4} \tag{20}$$

In Equation (18), the parameter k_{cell} is a measure of the apparent catalytic activity and will vary based on the actual catalyst surface area and the effective concentration of Hydrogen can be defined by a Henry's law equation of the form

$$C_{H2}^* = \frac{p_{H2}^*}{1.09 \times 10^6 \exp(\frac{77}{T})} \tag{21}$$

Further, Fowler et al. [8] introduced the degradation term in the equation (18) for ξ_2 to account for ageing, which is a factor affecting the durability of fuel cell stack. This term involves the apparent catalytic rate constants associated with the reactions on the anode and cathode side and changes in the catalytic active site density due to catalyst degradation.

$$\xi_2 = k_{DR} \times \frac{age}{T} + k_{cell} + 0.000197\ln(A) + 4.3 \times 10^{-5}\ln(C_{H2}^*) \tag{22}$$

Where, k_{DR} is the degradation rate of fuel cell due to the changes in catalytic activity and age is the ageing of the MEA in hours.

C. Ohmic overpotential

Every material has an intrinsic resistance to the flow of charge. The natural resistance of the material to the charge flow causes ohmic overpotential. The ohmic overpotential arises from the resistance of the polymer membrane to the transfer of protons and the resistance of the GDL, catalyst layer, bipolar plates and collector plates to the transfer of electrons.
The total ohmic overpotential is given by

$$\eta_{ohmic} = \eta_{ele} + \eta_{pro} = -I(R_{ele} + R_{pro}) \tag{23}$$

Where R_{ele} is the resistance to the transfer of electrons and R_{pro} is the resistance to the transfer of protons through the membrane. The electronic conductivity of the material is very high when compared to proton conductivity of the membrane and hence R_{ele} is neglected. The resistance of the membrane to the proton flow depends on the water content of the membrane, which further depends on temperature and current shown by Mann et al. [7].
A general expression for resistance to proton flow through the membrane is written as

$$R_{pro} = \frac{r_m \times l_m}{A} \tag{24}$$

Where r_m is the specific resistivity of the membrane for the flow of hydrated protons and is a function of the characteristics of the membrane type, current density, temperature and degree of hydration of the membrane.
The following empirical expression for the specific resistivity of the membrane is given by Fowler et al. [8]

$$r_m = \frac{181.6[1 + 0.03(I/A) + 0.062(T/30\ 3)^2(I/A)^{2.5}]}{[\lambda_{age} - 0.634 - 3(I/A)]\exp\{3.25[(T - 303)/T]\}} \tag{25}$$

Where λ is semi empirical parameter and is a function of the relative humidity and stoichiometric ratio of the anode and cathode, and also a function of age (time in service) of the membrane since the water carrying capacity of the membrane deteriorates with time in service.
 A simple linear relationship is proposed for the membrane conductivity degradation with age is

$$\lambda_{age} = \lambda^0 + \lambda_{DR} \times age \qquad (26)$$

Where λ^0 is initial membrane conductivity in terms of water content of the membrane, λ_{DR} is the membrane conductivity degradation rate, which varies with temperature and other operating conditions.

D. Concentration Overpotential

The concentration overpotential is caused by mass transport limitation of the reactants to the catalyst site, associated with electrochemical processes. Mass transport in fuel cell is mainly due to convection in channels and diffusion in electrodes. As soon as the fuel cell begins to produce current, the electrochemical reactions lead to depletion of reactants and accumulation of products at the catalyst layer. An empirical equation of the concentration overpotential is given by Guzzella [14]

$$\eta_{conc} = i(C_2 \frac{i}{i_{max}})^{C_3} \qquad (27)$$

Where C_2, C_3 and i_{max} are constants that depend on temperature and reactant partial pressure.

The coefficients in the equation are determined using nonlinear regression with polarization data from automotive propulsion PEM fuel cell stack as given by Pukrushpan $et\ al.$ [18] $C_3 = 2$, $i_{max} = 2.2$ and

if $\dfrac{p_{O_2}^*}{0.1173} + P_{H_2O} < 2atm,$

$$C_2 = (7.16 \times 10^{-4}\,T - 0.622)(\frac{p_{O_2}^*}{0.1173} + P_{H_2O}) + (-1.45 \times 10^{-3}\,T + 1.68) \qquad (28)$$

Else

$$C_2 = (8.66 \times 10^{-5}\,T - 0.068)(\frac{p_{O_2}^*}{0.1173} + P_{H_2O}) + (-1.6 \times 10^{-4}\,T + 0.54) \qquad (29)$$

E. Polarization Curves

The polarization curve of a fuel cell characterizes the cell voltage as a function of current density. At low current density region, the activation overpotential is more prominent due to slow rate of electron transfer. Whereas the ohmic overpotential is more prominent in the middle region of the polarization curve, since the proton conductivity of the membrane is less. At higher current density region, the amount of water produced in the cathode catalyst layer becomes greater than the amount of water that can be removed. Therefore, the electrochemical reactions within the catalyst layers are hindered by lack of reactants. Ultimately, these effects inhibit further reaction altogether and the cell voltage drops to zero (at limiting current density). However, the concentration losses can be mitigated by increasing the effective diffusivity or decreasing the GDL thickness.

F. Power Density

Power density is the product of output voltage and current density and hence increases with the current density as shown in Figure 12. After reaching the maximum value, power density starts decreasing since the rate of decrease in voltage is more than the rate of increase in current due to flooding of water at the catalyst sites and channels. The gross output power of the fuel cell is found as:

$$W_{Output} = i \times V \qquad (30)$$

G. Fuel Cell Efficiency

The efficiency of a fuel cell can be determined as the ratio of work output (electrical work) to the input energy which is the product of mass flow rate of hydrogen and its lower heating value.

$$E_{fc} = \frac{Work\ Output}{m_{H_2} \times LHV_{H_2}} \qquad (31)$$

The mass flow rate of hydrogen is correlated with the current as Larminie and Dicks [19]

$$m_{H_2} = \frac{(2.02 \times 10^{-3} \times I)}{2 \times F} \qquad (32)$$

Hence, the efficiency of fuel cell is

$$E_{fc} = \frac{I \times V}{\frac{(2.02 \times 10^{-3} \times I)}{2 \times F} \times LHV_{H_2} \times \gamma} \tag{33}$$

Where γ is anode stoichiometry.

IV. RESULTS AND DISCUSSIONS

A mathematical model is developed in the present work for the PEM fuel cell using semi empirical approach, simulated in the MATLAB environment and studied the effect of the operating parameters like temperature, membrane thickness and water content of the membrane on the performance of the fuel cell. Simulations were carried out by keeping the anode and cathode pressures at 3 bar and changing the cell temperatures from 315K to 345K, that being the range of the operating temperatures of PEM fuel cell. The thickness of the membrane is considered from 175 μm to 220 μm, since the Nafion 117 thickness as reported in the literature is from [7] 175-222 μm. The values of water content in the membrane, λ are varied from 14 to 20 as per Springer *et al.* [2] where the value of λ is taken as 22 under super saturated condition. For stationary fuel cell applications typically require more than 40,000 hours lifespan of reliable operation at a temperature of −35 °C to 40 °C, while automotive fuel cells require a 5,000 hour lifespan under extreme temperatures. Current service life is 7,300 hours under cycling conditions [20]. Therefore, age of the MEA for this study has been considered up to 6000 hours.

A. *Variation of overpotentials with various parameters*
Figure 2 shows the variation of activation overpotential with the current density at the mentioned pressure and various temperatures. The figure show that at low current draw, the activation overpotential is more pronounced due to the slow rate of electron transfer and a portion of the electrode voltage is lost in order to compensate for the lack of electro-catalytic activity.

As mentioned earlier, the beginning-of-life gas diffusion layer (GDL) loses its hydrophobicity over prolonged fuel cell operation and becomes more hydrophilic, causing voltage degradation. The total activation overpotential in the fuel cell is the sum of the contribution from anode and the cathode. The rate of reaction at
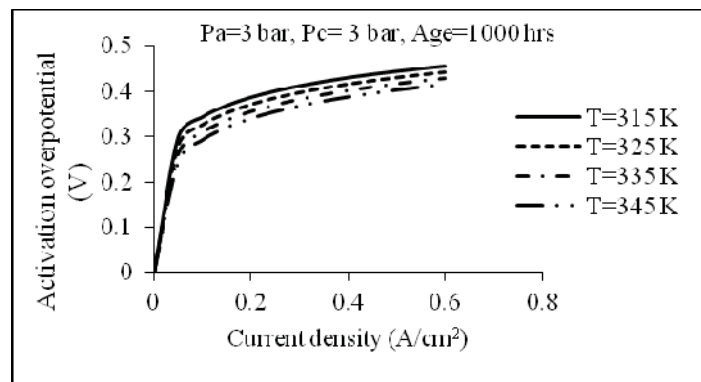

Fig.2 Activation overpotential as a function of current density at various operating temperatures.

equilibrium (exchange current density) is low at the cathode and hence the activation overpotential is highest at the cathode [16]. The anode and cathode exchange current densities depend on materials and porosity of the electrodes, concentration, distribution and dimensions of the catalyst particles and operating temperature of the fuel cell. Among these variables, the temperature is the only operating variable during fuel cell operation. As the temperature of fuel cell increases, there is a positive effect on the kinetic reaction rates and increase in the exchange current density will tend to reduce the activation overpotential.

It is seen from Figures 3 and 4, that the variation of ohmic overpotential with the current density is found to decrease with the increase in fuel cell temperature and water content (λ) in the membrane, respectively. Springer
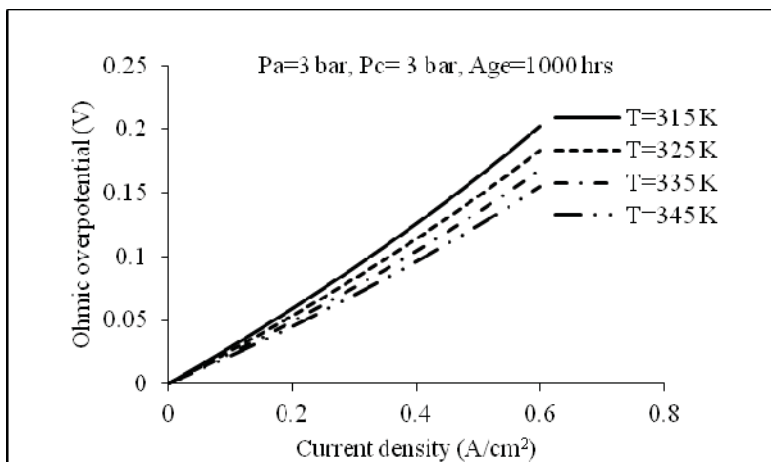
Fig. 3 Ohmic overpotential as a function of current density at various operating temperatures.
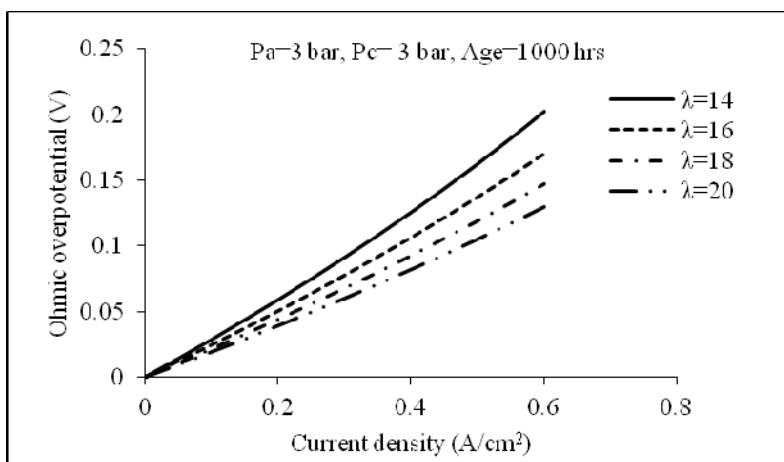

Fig.4 Ohmic overpotential as a function of current density at various levels of membrane water content.

et al. [2] proposed a semi-empirical expression to the proton conductivity of the membrane in terms of temperature of the fuel cell and membrane water content. At high temperatures, the membrane pores increase in diameter by absorbing more bulk-like water in the ionic clusters and hence increases the proton conductivity of the membrane. As the temperature increases, the electronic conduction in metals decreases, but the proton conductivity of polymers increases exponentially and these together decrease the ohmic overpotential. But in the present model, the affect of temperature on electronic conductivity has been neglected as mentioned earlier. Ohmic overpotential decreases with increasing water content of the membrane, since the proton conductivity depends on the water content.
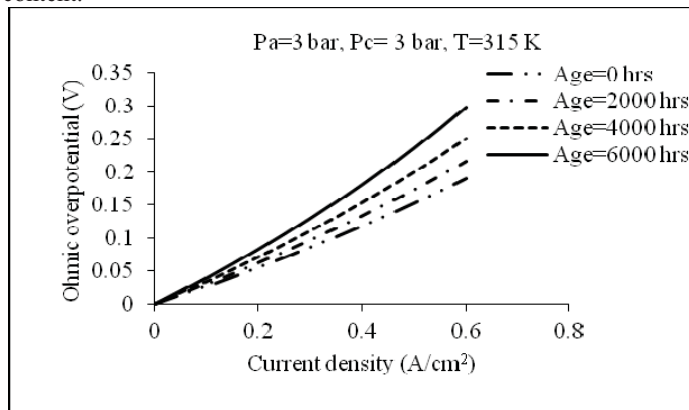

Fig.5 Ohmic overpotential as a function of current density at various operating hours of the MEA.

The variation of ohmic overpotential with current density at various ageing time or time in service of the MEA has also been studied as shown in Figure 5. The water carrying capacity of the membrane deteriorates with time

in service which is directly proportional to the proton conductivity of the membrane. Therefore, the ohmic overpotential decreases with ageing of the membrane. Generally, the ohmic overpotential is present at all current densities since the proton conductivity of the membrane is very less.
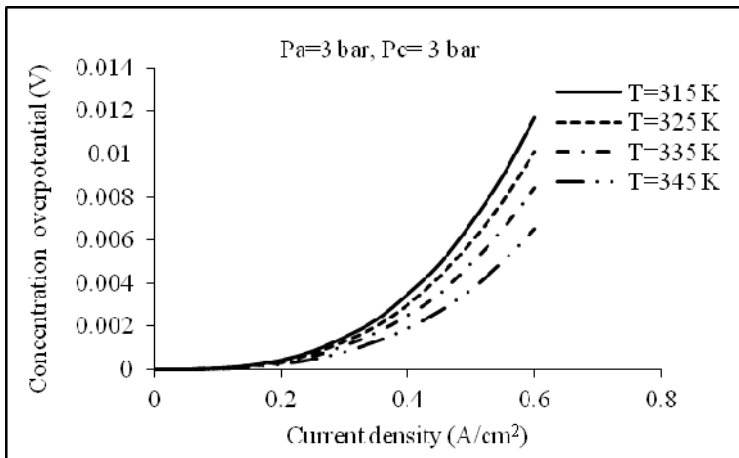

Fig.6 Concentration overpotential as a function of current density at various operating temperatures

The variation of concentration overpotential as a function of current density at various operating temperatures is shown in Figure 6. It is seen that, at low current density, the concentration losses are almost zero since the water production is negligible. As the current density increases, the product accumulates at the catalyst sites and gas flow channels which hinder the mass transport of reactants to the sites, increasing the concentration overpotential. As the temperature increases, water accumulation at the gas channels and catalyst sites decreases which results in decreasing the concentration overpotential.

B.   Effect of various operating parameters on the Polarization curves
Figures 7 - 10 represents the polarization curves with varying operating temperatures, membrane thicknesses and different operating anode and cathode pressures respectively which have been developed from the model. Polarization curves shifts towards the higher side of output voltage with increase in temperature since the exchange current density and proton conductivity increase with the cell temperature. The water accumulation at the gas channels and catalyst sites decreases with increase in cell temperature reducing the overpotentials as shown in Figure 7.
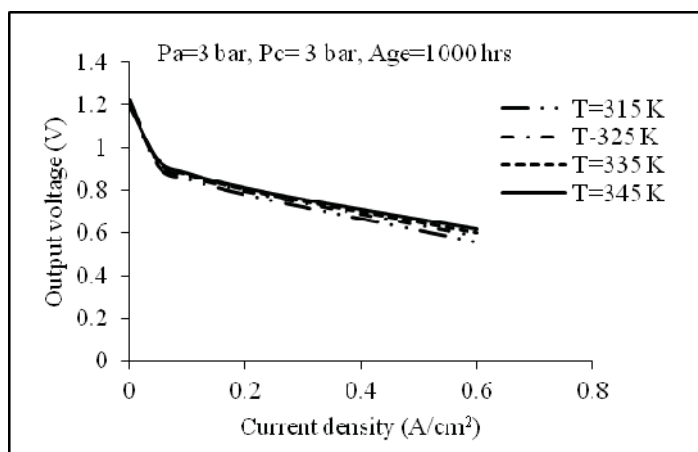

Fig.7 Polarization curves at various operating temperatures.

The ohmic overpotential decreases, with decrease in the thickness of the membrane as thinner membranes will enhance back diffusion from cathode to anode. The back diffusion from the cathode will keep anode electrode saturated, preventing anode dehydration at higher current densities. Hence, decrease in ohmic overpotential would result in the increase of the output voltage with the decrease in the thickness of the membrane as observed in Figure 8. Thinner membranes are advantageous for PEM fuel cells. Fuel cell polarization curves typically increase with increasing operating pressures as seen in Figures 9 and 10 due to the increased rate of chemical
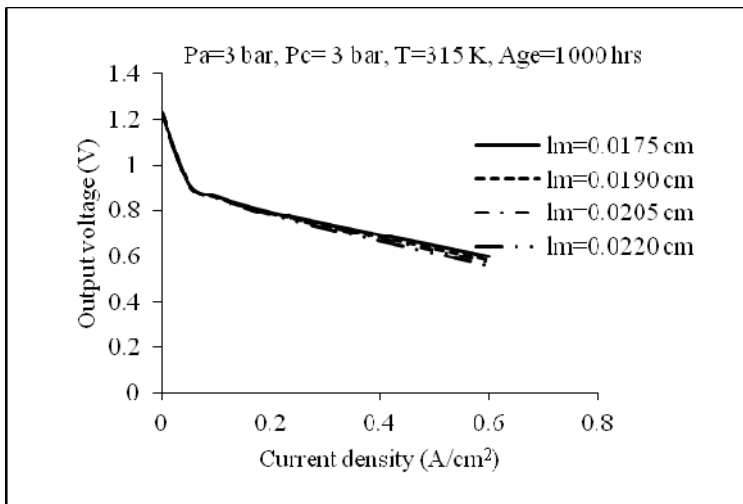
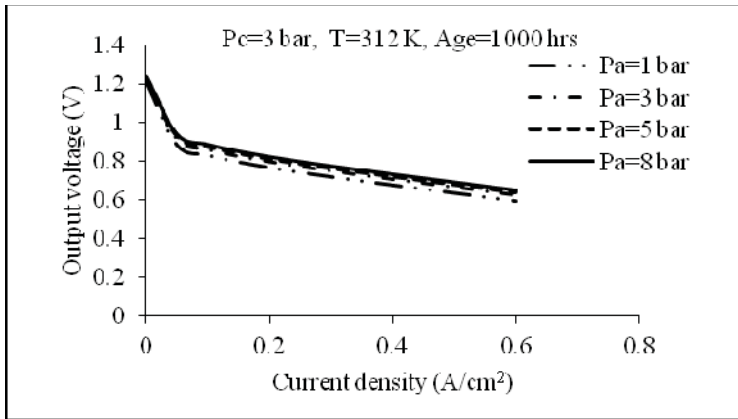Fig.8 Polarization curves at various membrane thicknesses.

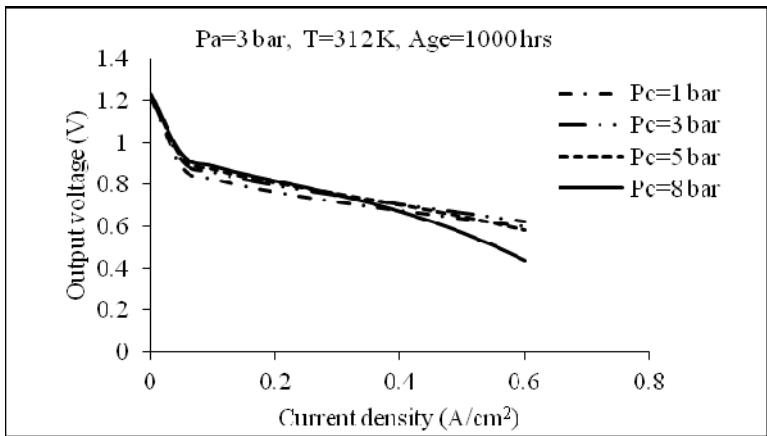Fig.9 Variation of polarization curves with change in anode pressure.

Fig.10 Variation of polarization curves with change in cathode pressure.

reaction which is proportional to the partial pressures of hydrogen and the oxygen. High pressures forces hydrogen and oxygen to come into contact with the electrolyte. However, the output voltage of the fuel cell is changed from 0.59 V to 0.624 V at a current density 0.6A/cm^2 when cathode and anode pressures increase from 1 to 3 bar, above this pressure the change in output voltage is insignificant. Also, Figure 10 shows that, beyond a cathode pressure of 8 bar, there is a sudden drop in voltage at the current density above 0.3 A/cm^2. This might be due to the process of flooding which takes place above this region due to concentration overpotential. It is always desirable to keep both anode and cathode at the almost same pressures to avoid damage of the cell membrane due to pressure difference.

C. *Validation of the present model results with the experimental data*

Table 1 Parameters of the fuel cell used in the model for validation

| Parameter	Value
Anode pressure (P_{H2})	3 bar
Cathode pressure (P_{air})	3 bar
Active area of the fuel cell (A)	100 cm^2
Membrane thickness (l_M)	0.0220 cm [7]
Water content in the membrane (λ)	14 [2]
Operating time	1000 hrs
Degradation rate of fuel cell due to changes in catalytic activity (k_{DR})	-0.055 µVK/h [8]
Activity term (k_{cell})	0.00295 [8]
Membrane conductivity degradation rate (λ_{DR})	-0.0007/h [8]
Constant used in concentration overpotential (i_{max})	2.2 [18]
Constant used in concentration overpotential (C_3)	2 [18]
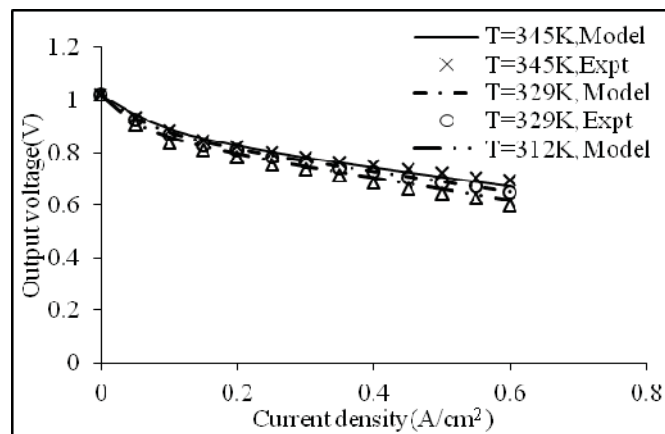
Fig.11 Validation of the polarization profiles for model result with experimental data [15].

The present results obtained from the modelling has been validated with the experimental results of Ballard MK5-E proton exchange membrane fuel cell (PEMFC) stack at various temperatures presented by Laurencelle *et al.* [15]. The parameters used for the model validation is presented in the Table 1.

Figure 11 presents the comparison of the polarisation curve drawn from the model result and with the experimental data [15] at three different temperatures of 312 K, 329 K and 345 K. An excellent agreement has been demonstrated between the model results and the experimental results and the trends of polarization curves are also quite similar. However, experimental values at 312K are slightly lower than the predicted model values but the trend of the polarization curve is similar. One plausible source of this deviation might be at the lower temperature and higher current densities; the product accumulates at the catalyst sites and gas flow channels which hinder the mass transport of reactants to the sites, increasing the concentration overpotential and some other system parameters are not well defined in the literature.

D. *Variation of power density as a function of current density at various parameters*

Figure 12 shows the variation of power density as a function of current density at various temperatures of the fuel cell. The maximum power density increases with the temperature since the overpotentials decrease with temperature. The power density will increase with the increase in temperature of the fuel cell due to the positive effect on kinetic reaction rates increasing the exchange current density. Also, with increase in the temperature, proton conductivity of the membrane will increase tending to decrease the overpotential. The maximum power density also shifts towards right along the higher current density, since by increasing the temperature of the fuel cell, the rate of water removal is enhanced at the cathode membrane interface, delaying the flooding of water at the catalyst sites. The cell voltage at maximum power density varies from 0.46 V to 0.5 V.
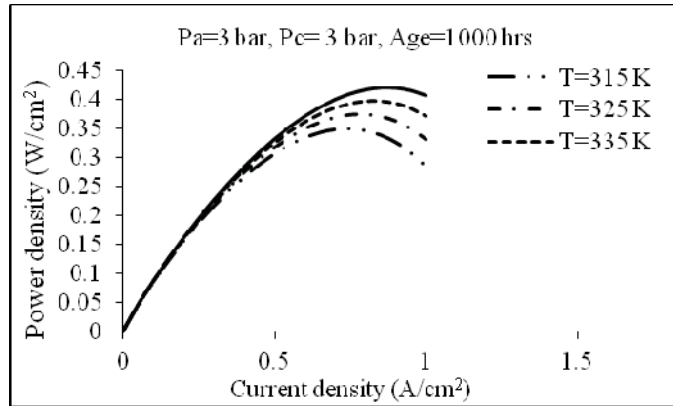
Fig.12 Power density as a function of current density at various temperatures

Figure 13 shows the variation of power density with the current density for various operating hours of the MEA. The beginning-of-life GDL exhibits hydrophobic characteristics and over prolonged fuel cell operation becomes hydrophilic as described earlier, causing voltage degradation. Hence, the water carrying capacity of the membrane deteriorates with time in service which is directly proportional to the proton conductivity of the membrane. Therefore, the ohmic overpotential decreases with ageing of the membrane and both losses together
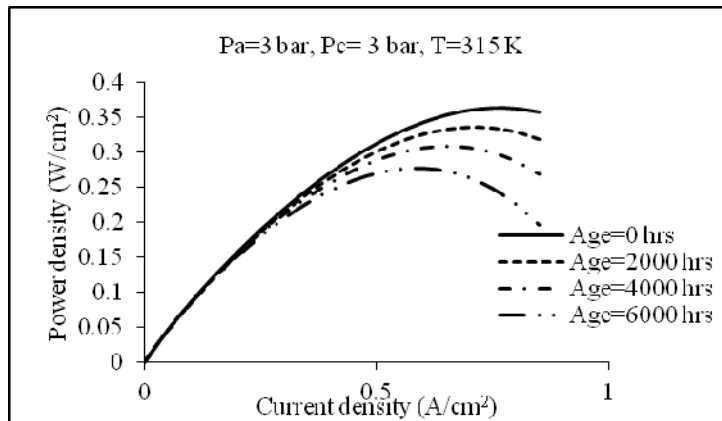

Fig.13 Power density as a function of current density at various operating hours of the MEA

reduce cell voltage and hence power density. The cell voltage at maximum power density degrades from 0.62 V to 0.54 V at a current density 0.5 A/cm^2 with the operating time of the MEA. Also, the maximum power density points shifts towards the left along the higher current density, because with the increase in ageing of the MEA, the mobility of species within the chain also decreases reducing the diffusion coefficient for water transport and hence the water removal rate is less at the cathode membrane interface, advancing the flooding of water at the catalyst sites. Hence, it should be noticed that it's never desirable to operate the fuel cell in the range beyond where the power curve drops off.

Fig.14 Efficiency as a function of current density at various temperatures

Figure 14 shows the variation of efficiency of fuel cell with the current density for various temperatures and it is noticed that the efficiency increases with temperature since the output voltage is directly proportional to the fuel cell efficiency. The efficiency of fuel cell is modelled at an anode stoichiometry of 1.4 because of internal current loss and fuel cross over is more in case of Nafion membranes which are presently used in PEM fuel cells. Insufficient stoichiometry deprives the fuel cell stack of sufficient reactants and may cause permanent damage. As the stoichiometry increases, more contact of gas molecules takes place so that efficiency of fuel cell increases. It is found that the fuel cells should be practically operated at an anode stoichiometry of 1.4.

V. CONCLUSION

A mathematical model has been developed in the present work for the PEM fuel cell using semi empirical approach, simulated in the MATLAB environment and studied the effect of the operating parameters like temperature, membrane thickness, anode and cathode pressures and physical ageing of the MEA on the performance of the fuel cell. The variation of overpotentials with the temperature of the fuel cell and ohmic overpotential with respect to the water content of the membrane and physical ageing of the MEA has also been studied. The following conclusions could be drawn based on the results:

- The effect of temperature on the performance of the fuel cell is more significant as compared to the other parameters. Even though the increase in fuel cell temperature reduces the Gibb's free energy of the reaction, the performance of fuel cell increases. This is because of three reasons, firstly, the exchange current density increases with the temperature reducing the activation overpotential, secondly, the increase in proton conductivity with temperature reduces ohmic overpotential and thirdly, the limiting current density of the fuel cell increases indicating enhancement in mass transport due to the increase of diffusivity reducing the concentration overpotential.
- Thinner membranes will enhance back diffusion from cathode to anode preventing anode dehydration at higher current densities. Hence, with the decrease in the thickness of the membrane there would be a decrease in ohmic overpotential resulting in the increase of the output voltage.
- It was found that the effect of anode and cathode gas pressures is quite significant up to a pressure of 3 bar on the output voltage of the fuel cell, above which the effect is negligible.
- The power density is found to be decreasing with ageing of the MEA as both the catalytic activity and proton conductivity of the membrane decreases. The limiting current density also decreases with ageing since water removal rate at the catalyst sites decreases, advancing the flooding of water.

For commercial applications, the end-of-life (EOL) performance is of great interest, the model can be extended over the life of a fuel cell so that performance could now be predicted as the fuel cell ages. Hence, this model could be an extremely useful tool for the design analysis of PEM fuel cell power systems without extensive calculations over the life of a fuel cell. However, this model does not account for the impact of operation in poorly hydrated manner where λ is less than 14, which will affect the voltage degradation rate with ageing of the fuel cell.

Nomenclature

A	cell active area, cm^2
age	operating time, hours
C_i	concentration of species i, mol/cm^3
E	open circuit voltage, V
E_0	reference voltage, V
F	Faraday's constant, 96487 C/equi
ΔFe	standard state of free energy of activation for the reaction, J/mol
ΔFec	standard state of chemisorptions from the gas state, J/mol
I	current, A
i	current Density, A/cm^2
ka^0, k_c^0	intrinsic rate constants for the anode and cathode reactions respectively, cm/s
k_{cell}	empirical term accounting for the apparent rate constants for the anode and cathode reactions
k_{DR}	empirical term representing the ageing in the overall catalytic activity, $Vh^{-1}K^{-1}$
l_m	thickness of polymer membrane, cm
LHV_{H2}	lower heating value of Hydrogen, J/kg
m_{H2}	mass flow rate of hydrogen, kg/s
n	number of equivalents involved in a reaction
P_c	cathode gas pressure, bar
P_a	anode gas pressure, bar
P_{H2O}	saturation pressure of water, atm. for Eqs. 7,8,28 & 29, bar for eq. 9
p_i	partial pressure of species i, atm

r_m	membrane specific resistivity for the flow of hydrated protons, ohm cm
R	gas constant, 8.3143 J/mol-K
t	fuel cell temperature, ^{o}C
T	fuel cell temperature, K
V	output voltage, V

Greek letters

λ	semi-empirical parameter representing the effective water content of the membrane, H_2O/SO_3^-
λ_{DR}	empirical parameter representing the ageing of the polymeric membrane, h^{-1}
α_c	chemical activity parameter for the cathode
η_{act}	activation overpotential
η_{ohmic}	ohmic overpotential
η_{conc}	concentration overpotential
$\xi_1, \xi_2, \xi_3, \xi_4$	semi-empirical coefficients for calculation of activation overpotential

REFERENCES

[1] Holber, M., A. Carlsson, P. Johansson, L. Jorissen, and P.Jacobsson, Raman investigation of degradation and ageing effects in fuel cell membranes, *ECS Transactions,* 25 (2009) 807-11.

[2] Springer, T.E., T.A.Zowodzinski, and S. Gottesfeld. Polymer Electrolyte Fuel Cell Model, *Journal of The Electrochemical Society,* 138 (1991) 2334-42.

[3] Bernardi, D.M., and M.W. Verbrugge, A Mathematical Model of the Solid Polymer Electrolyte Fuel cell, *Journal of The Electrochemical Society,* 139 (1992) 2477-91.

[4] Amphlett, J.C., R.M. Baumert, R.F.Mann, B.A. Peppley, P.R.Roberge, and T.J.Harris, Performance Modeling of the Ballard Mark IV Solid Polymer Electrolyte Fuel Cell: I Mechanistic Model Development, *Journal of The Electrochemical Society,* 142 (1995) 1-8.

[5] Amphlett, J.C., R.M. Baumert, R.F.Mann, B.A. Peppley, P.R.Roberge, and T.J.Harris, Performance Modeling of the Ballard Mark IV Solid Polymer Electrolyte Fuel Cell: II Empirical Model Development, *Journal of The Electrochemical Society,* 142 (1995) 9-15.

[6] Kim, J., S. Lee, and S. Srinivasan, Modeling of proton exchange membrane fuel cell performance with an empirical equation, *Journal of The Electrochemical Society,* 142 (1995) 2670–74.

[7] Mann, R.F., J. C. Amphlett, M. A.I. Hooper, H. M. Jensen, B.A. Peppley, and P. R. Roberge, Development and application of a generalised steady-state electrochemical model for a PEM fuel cell, *Journal of Power Sources,* 86 (2000) 173-80.

[8] Fowler, W., F. Mann, J. C. Amphlett, B. A. Peppley, and P. R. Roberge, Incorporation of voltage degradation into a generalised steady state electrochemical model for a PEM fuel cell, *Journal of Power Sources,*106 (2002)274-83.

[9] Maxoulis, C.N., D. N. Tsinoglou, and G. C. Koltsakis, Modeling of automotive fuel cell operation in driving cycles, *Energy Conversion and Management,* 45 (2004) 558-73.

[10] Al-Baghdadi, M.A.R.S., Modelling of proton exchange membrane fuel cell performance based on semi-empirical equations, *Renewable Energy,* 30 (2005) 1587-99.

[11] Youssef, M.E., K. E.AL-NAdi, and M. H. Khalil, Lumped Model for Proton Exchange Membrane Fuel Cell (PEMFC), *International Journal of Electrochemical Science,* 5 (2010) 267-77.

[12] Mert, S.O., I.Dincer, and Z.Ozcelik, Performance investigation of a transportation PEM fuel cell system, *International Journal of Hydrogen Energy,* 37 (2012) 623-33.

[13] Sperling, L.H., *Introduction to physical polymer science,* (John Wiley &Sons Inc., New York) 1992.

[14] Guzzella, L., Control Oriented Modeling of fuel cell based Vehicles, *Presentation in NSF Workshop on the integration of modeling and control for Automotive Systems,* Santa Barbara, 5-6 June 1999.

[15] Laurencelle, F., R. Chahine, J. Hamelin, K. Agbossou, M. Fournier, T. K. Bose, and A. Laperrire, Characterization of a Ballard MK5-E Proton Exchange Membrane Fuel Cell Stack, *Fuel cells,* 1 (2001) 66-71.

[16] O'Hayre, R., S.W. Cha, W. Colella, and F.B. Prinz, *Fuel Cell Fundamentals,* 2nd edn, (John Wiley & Sons, New York) 2009.

[17] Spiegel, C. Mathematical modelling of polymer exchange membrane fuel cells. PhD diss., University of South Florida, 2008.

[18] Pukrushpan, J.T., A. G. Stefanopoulou, and H. Peng, Modeling and Control for PEM Fuel Cell Stack System, *Paper presented at the American Control Conference*, Anchorage, 8-10 May 2002.

[19] Larminie, J., and A. Dicks, *Fuel cell Systems explained,* 2nd edn, (John Wiley & Sons Ltd. England) 2003.

[20] Wikipedia, https://en.wikipedia.org/wiki/Fuel_cell, August 1, 2013.